N-phonon giant resonances in the nonlinear hydrodynamic approach and the nucleon-nucleon interaction

V. Yu. Denisov*
Institute for Nuclear Research, Prospect Nauki 47, 252028 Kiev, Ukraine
(Received 29 May 1997)

Isoscalar and isovector density vibrations in a slab with sharp edges are studied in a nonlinear hydrodynamic approach. The frequency shift of the N-phonon excitation due to nonlinear terms is obtained. The frequencies of one- and two-phonon vibrations calculated in the nonlinear hydrodynamic theory are reduced by $\approx 5-30$ % for isoscalar and by $\approx 1-8$ % for isovector resonances as compared to the linear approximation. The frequency shift is a function of both the slab thickness and the parameters of the nucleon-nucleon interaction. Experimental data on the frequency shift of the N-phonon states due to the nonlinear terms in the case $N \geqslant 2$ may be used for selecting of the set of nucleon-nucleon interaction parameters. [S0556-2813(98)01902-5]

PACS number(s): 21.60.Ev, 21.65.+f, 24.10.Nz, 24.30.Cz

I. INTRODUCTION

Giant dipole resonances were predicted [1] and experimentally discovered [2] more than 50 years ago. Nevertheless giant resonances have been and still are a major topic of research in nuclear physics [1–15]. Many different types of giant resonances have been discovered [5,6]. In the past few years two-phonon giant resonances have been studied both experimentally and theoretically [10,12–15]. The two-phonon giant dipole resonance has been observed at an energy approximately twofold larger than that of the one-phonon resonance [12,14].

The one-phonon giant resonance is treated as the excited state built on the ground state of the nucleus. In the framework of the harmonic oscillator model the two-phonon giant resonance is treated as the excited state built on the one-phonon excitation. Decay schemes of the one- and two-phonon giant resonances confirm the origin of these resonances [12,14,15]. The N-phonon state may also be considered in a similar way. Therefore the energy of the N-phonon giant resonance $E_{N\hbar\omega}$ must be N-fold larger than the energy of one-phonon giant resonance $E_{1\hbar\omega}$ using a harmonic oscillator model assumption. However, the measured energies of the two-phonon isovector giant dipole resonances are slightly smaller than $2E_{1\hbar\omega}$ [12,14]. Such a reduction in the excitation energy of the two-phonon state is caused by the anharmonicity of vibrations in the nuclear matter.

The purpose of this paper is to study the frequency shift of the N-phonon isoscalar and isovector vibrational states due to the anharmonicity of density oscillations in a slab of nuclear matter with sharp edges in the framework of the nonlinear hydrodynamic model. We will attempt to obtain an analytical expression for the frequency shift of the N-phonon isoscalar and isovector resonances caused by the vibrations nonlinearity. Therefore we consider giant resonances in a slab with sharp edges. It should be noted that various properties of giant resonances have been successfully described using different linear hydrodynamic approximations [3,4,6–8].

The anharmonicity of the two-phonon giant resonances was estimated in the schematic nonlinear random-phase approximation (RPA) model with a simplified interaction in [10]. The nonlinearity of one-phonon isoscalar monopole giant resonance was investigated in the relativistic mean field theory [9]. Both of these studies require cumbersome numerical calculations and the link between the parameters of the nucleon-nucleon interaction and the shift of resonance energy caused by anharmonicity is obtained numerically.

The analytical expression derived in this paper confirms the direct and transparent connection between the shift of energy of the N-phonon giant resonances due to anharmonicity and the constants of the Skyrme-type [17,18] energy density functional. The constants of the energy density functional are related the parameters of nucleon-nucleon interaction [17,18].

The nonlinear hydrodynamic model of the density vibrations in the slab of nuclear matter is described in Sec. II. The results for isoscalar and isovector excitations are presented in Secs. III and IV, respectively. The summary and conclusions are presented in Sec. V.

II. NONLINEAR DENSITY VIBRATIONS IN A SLAB

Density oscillations $\rho(r,t)$ in the hydrodynamic approximation are described by the continuity equation [16]

$$\frac{\partial\rho}{\partial t}+\mathrm{div}(\rho\mathbf{v})=0 \tag{1}$$

and the Euler equation

$$\frac{\partial\mathbf{v}}{\partial t}+(\mathbf{v}\nabla)\mathbf{v}+\frac{1}{m}\nabla\frac{\delta\mathcal{E}(\rho)}{\delta\rho}=0, \tag{2}$$

where $\mathbf{v}(r,t)$ is the velocity of nucleons and $\delta\mathcal{E}(\rho)/\delta\rho$ is the variational derivative of the energy density functional.

Let us consider the energy density functional of nuclear matter of the form

*Electronic address: denisov@kinr.kiev.ua

$$\mathcal{E}(\rho)=\mathcal{E}(\rho_\infty)+a_0\frac{(\rho-\rho_\infty)^2}{2\rho_\infty}+b_0\frac{(\rho-\rho_\infty)^3}{6\rho_\infty^2}+c_0\frac{(\rho-\rho_\infty)^4}{12\rho_\infty^3}+d_0\frac{(\nabla\rho)^2}{2\rho_\infty}, \tag{3}$$

where $a_0,\ b_0,\ c_0,\ d_0$ are constants. We should note that the form of realistic energy density functionals [17,18] does not coincide exactly with Eq. (3). However, any realistic functional may be expanded into a series in the deviation of density from the equilibrium value ρ_∞ as in Eq. (3), when there are no gradient terms. The form of the gradient term in Eq. (3) is the same as the form of the gradient term of the energy density functional of Skyrme force in the Thomas-Fermi approach [17,18].

The spatial distribution of nuclear matter in the slab is confined along the z axis between $-R$ and R and is infinite along the x and y axes of the Cartesian system of coordinates. The energies of different giant resonances are proportional to the nucleus radius or $A_N^{-1/3}$ [5,6], where A_N is the mass number. In the case of the slab the z axis simulates the radial coordinate of the spherical system of coordinates. The role of the slab's x and y coordinates is considered to be similar to the role of angular coordinates in a spherical system of coordinate for nuclei.

Given a slab geometry, Eqs. (1) and (2) may be simplified:

$$\frac{\partial\xi}{\partial t}+\frac{\partial v}{\partial z}+f\frac{\partial\xi v}{\partial z}=0, \tag{4}$$

$$\frac{\partial v}{\partial t}+a\frac{\partial\xi}{\partial z}-d\frac{\partial^3\xi}{\partial z^3}+ev\frac{\partial v}{\partial z}+b\xi\frac{\partial\xi}{\partial z}+c\xi^2\frac{\partial\xi}{\partial z}=0, \tag{5}$$

where $a=a_0/m,\ \ b=b_0/m,\ \ c=c_0/m$, and $d=d_0/m$, e and f are the auxiliary constants ($e=f=1$), and ξ is the function described by the density vibrations

$$\rho(z,t)=\rho_\infty[1+\xi(z,t)]. \tag{6}$$

Equations (4) and (5) are nonlinear. The nonlinear terms which contain constants e and f in Eqs. (4) and (5) arise due to the nonlinear nature of the hydrodynamic equations. The terms with constants b and c in Eqs. (4) and (5) are related to the anharmonic potential nature of the energy density functional (3).

Let us try to solve the system of equations (4) and (5) in the form of the perturbation series which is often similar to the treatment of the nonlinear oscillations in classical mechanics [23]:

$$\xi=\xi_0+\xi_1+\xi_2+\cdots, \tag{7}$$

$$v=v_0+v_1+v_2+\cdots, \tag{8}$$

$$k=k_0+k_1+k_2+\cdots, \tag{9}$$

$$\omega=\omega_0+\omega_1+\omega_2+\cdots. \tag{10}$$

In first approximation the solution of Eqs. (4) and (5) is

$$\xi_0=\alpha\sin(\omega_0 t)\sin(k_0 z+\varphi), \tag{11}$$

$$v_0=\alpha\frac{\omega_0}{k_0}\cos(\omega_0 t)\cos(k_0 z+\varphi). \tag{12}$$

Here α is the vibrations amplitude and ω_0 and k_0 are the frequency and the wave vector of the oscillations, respectively. We choose the solution of Eqs. (4) and (5) in the form (11) and (12) because this solution exists in the case $d\to 0$ and describes ordinary sound waves. The solutions obtained in the first order of perturbation theory are linear in α. The frequency and wave vector are connected by the dispersion equation

$$\omega_0^2=ak_0^2+dk_0^4. \tag{13}$$

As we have noted, the z coordinate for the slab geometry corresponds to the radial coordinate r of the spherical nucleus. The transition densities of the giant resonances of the multipolarity $\ell\geqslant 1$ are equal to zero at the center of the spherical nucleus $z=r=0$ [6–8]. In contrast to this, transition densities of the monopole giant resonances have a finite amplitude of vibrations at the center of the nucleus [4,8]. Therefore we may simulate the transition densities of different behavior at $z=0$ by choosing the value of the phase φ in Eqs. (11) and (12). The values of the phase $\varphi=0$ and $\varphi=\pi/2$ modulate the transition densities of the giant resonances with multipolarities $\ell\geqslant 1$ and $\ell=0$, respectively. The results of this section do not depend on the choice of phase, so we assume $\varphi=0$ for the sake of simplicity.

The wave vector k_0 of density oscillations is determinated by linear boundary conditions on the free surfaces of the slab. The boundary conditions are discussed in detail in the next sections. Due to the dispersion relation (13) the frequency of vibrations ω_0 is also fixed by the boundary conditions. The amplitude of vibrations is obtained from the condition of energy equality, evaluated by means of the quantum and classical expressions

$$\hbar\omega_0=E_{\mathrm{class}}. \tag{14}$$

The vibrations energy calculated in the classical approach is

$$E_{\mathrm{class}}=\frac{1}{2}\int dVm\rho_\infty v_0^2+\int dV\rho_\infty\left(a_0\frac{\xi_0^2}{2}+d_0\frac{(\nabla\xi_0)^2}{2}\right). \tag{15}$$

Note that $E_{\mathrm{class}}\propto\alpha^2$.

The nuclear interaction within the slab volume is much stronger than on its surfaces. Therefore we may consider that the nonlinear density vibrations dynamics in the slab are determined by the dynamics within the slab, and that the oscillations of surfaces are tuned up on the volume dynamics. We shall ignore the nonlinearities in the boundary conditions. One can see that we should take into account $\hbar^2$ and $\hbar^4$ corrections to the Thomas-Fermi kinetic energy [18] in order to describe accurately the surface layer of nuclear matter. We have limited ourselves to the Thomas-Fermi approach to kinetic energy functional in Eq. (3). So, we fixed the wave vector k in the next orders of perturbation theory to be the same as in the linear approximation, i.e., $k=k_0$.

The terms with coefficients b, e, and f of Eqs. (4) and (5) should be taken into account in the second order perturbation analysis. The system of equations for determining ξ_1 and v_1 is given by

$$\frac{\partial \xi_1}{\partial t}+\frac{\partial v_1}{\partial z}=-f\frac{\partial(\xi_0 v_0)}{\partial z}, \tag{16}$$

$$\frac{\partial v_1}{\partial t}+a\frac{\partial \xi_1}{\partial z}-d\frac{\partial^3 \xi_1}{\partial z^3}=-ev_0\frac{\partial v_0}{\partial z}-b\xi_0\frac{\partial \xi_0}{\partial z}. \tag{17}$$

By taking the time derivative of Eq. (16) and the derivative with respect to z of Eq. (17) and subtracting Eq. (17) from Eq. (16) we obtain the equation for ξ_1

$$\frac{\partial^2 \xi_1}{\partial t^2}-a\frac{\partial^2 \xi_1}{\partial z^2}+d\frac{\partial^4 \xi_1}{\partial z^4}=2\alpha\omega_0\omega_1\sin(\omega_0 t)\sin(kz) -\frac{1}{2}\alpha^2\{\cos(2\omega t)[(2f+e)\omega_0^2 +bk^2]+(e\omega_0^2-bk^2)\}\cos(2kz). \tag{18}$$

The condition that there be no resonance term [23] on the right side of this equation leads to $\omega_1=0$. Equations (16)–(18) can be solved as

$$\xi_1(z,t)=\alpha^2[A\cos(2\omega_0 t)+B]\cos(2kz), \tag{19}$$

$$v_1(z,t)=\alpha^2\frac{\omega_0}{k}(A-f/4)\sin(2\omega_0 t)\sin(2kz), \tag{20}$$

where

$$A=\frac{(2f+e)\omega_0^2+bk^2}{8(\omega_0^2-ak^2-4dk^4)}, \quad B=\frac{bk^2-e\omega_0^2}{8(ak^2+4dk^4)}. \tag{21}$$

By using the same method as before we may easily obtain the third order solution. The nonresonance term condition [23] in this order of the perturbation theory leads to the finite correction of the oscillation frequency

$$\omega_2\equiv\omega_{\text{shift}}(b,c,e,f) =\frac{-\alpha^2}{192(a+dk^2)^{1/2}(a+4dk^2)dk}\{a^3(4f^2+4ef+e^2) +a^2b(4f+2e)+ab^2+[6a^2(e^2+6ef+5f^2)+a(4be -18c+14bf)+10b^2]dk^2+[a(9e^2+78ef+66f^2) +2be+10bf-72c]d^2k^4 +(4e^2+46fe+40f^2)d^3k^6\}. \tag{22}$$

The vibration frequency changes in third order perturbation theory. This frequency shift of oscillations ω_{shift} is proportional to the square of amplitude of vibrations, see also [23].

The energy of the one-phonon $(1\hbar\omega)$ giant resonance connected with density vibrations in the slab of nuclear matter is equal to

$$E_{1\hbar\omega}=\hbar[\omega_0+\omega_{\text{shift}}(b,c,1,1)]. \tag{23}$$

Here we have taken into account the semiclassical quantization rule for the classical periodic motion.

The N-phonon giant resonance in the slab is defined as coherent excitation of N one-phonon oscillations. The density fluctuation of the N-phonon giant resonance may be presented as

$$\xi_{N\hbar\omega}(z,t)=\alpha\sin(\omega_0 t)\sin(k_0 z)+\alpha\sin(\omega_0 t)\sin(k_0 z)+\cdots +\alpha\sin(\omega_0 t)\sin(k_0 z) =(N\alpha)\sin(\omega_0 t)\sin(k_0 z). \tag{24}$$

Thus, the vibration amplitude of the N-phonon excitation is by N-fold larger than the amplitude of the one-phonon state. The N-phonon density oscillations in the slab are also described by the system of hydrodynamic expressions (4) and (5). The frequency shift of the N-phonon excitation due to anharmonicity can be easily determined from the expressions for the one-phonon case by substituting the constants related with the nonlinear terms of Eqs. (4) and (5):

$$b_{N\hbar\omega}\to Nb_{1\hbar\omega}, \quad c_{N\hbar\omega}\to N^2c_{1\hbar\omega}, \quad e_{N\hbar\omega}\to Ne_{1\hbar\omega}=N, \quad f_{N\hbar\omega}\to Nf_{1\hbar\omega}=N. \tag{25}$$

Therefore the energy of the N-phonon excitation is given by

$$E_{N\hbar\omega}=\hbar[N\omega_0+\omega_{\text{shift}}(Nb,N^2c,N,N)]. \tag{26}$$

Let us define the ratios of energies V_N and W_{NM} as

$$V_N=\frac{E_{N\hbar\omega}-N\hbar\omega_0}{\hbar\omega_0}=\frac{\omega_{\text{shift}}(Nb,N^2c,Ne,Nf)}{\omega_0}, \tag{27}$$

$$W_{NM}=\frac{E_{N\hbar\omega}-E_{M\hbar\omega}}{E_{M\hbar\omega}} =\approx\frac{N-M}{M}\left(1+\frac{M\omega_{\text{shift}}(Nb,N^2c,N,N)-N\omega_{\text{shift}}(Mb,M^2c,M,M)}{M(N-M)\omega_0}\right). \tag{28}$$

The ratios V_N and W_{NM} quantify the nonlinearity (or anharmonicity) of the N-phonon excitation and the relative anharmonicity of the N-phonon and the M-phonon states, respectively. These ratios are equal to $V_N=0$ and $W_{NM}=(N-M)/M$ in the case of harmonic oscillations. Deviations from these limiting values give us the qualitative characteristics of the anharmonicity.

The ratio V_N has only useful theoretical applications. We must emphasize that the ratio W_{NM} can be derived from experimental data. Moreover, experimental data on the ratio W_{21} for the electric giant dipole resonance can be found in [12,14]. The ratios V_1 and W_{21} will be analyzed in detail for isoscalar and isovector vibrations in Secs. III and IV, correspondingly.

III. ISOSCALAR EXCITATION

The proton and neutron densities vibrate in phase in the case of isoscalar oscillations. These vibrations are described by Eqs. (4) and (5) and satisfy kinematic and dynamic boundary conditions on the free surfaces of the slab at $z=\pm R$ [7,8].

The kinematic boundary condition assumes to be equality of the normal to the surface velocities of the nucleons $v(z,t)$ to the surface $v_{S\pm}(t)$, i.e.,

$$v(z,t)|_{z=\pm R}=v_{S\pm}(t), \tag{29}$$

where $v_{S\pm}(t)=\partial\delta_{\pm}(t)/\partial t$ is the velocities of surfaces of the slab and $\delta_{\pm}$ is the amplitude of surfaces oscillation. Here and below the subscripts + and − denote the right $(z=R)$ and the left $(z=-R)$ surfaces of the slab, respectively.

The dynamic boundary condition is assumed to be the equality of the normal to the surface pressure $\sigma(z,t)$ caused by the distortion of nucleon density $\xi(z,t)$ within the slab to the pressure $P_{\pm}(t)$ caused by the restoring force of the surface at the shift of surface $\delta_{\pm}$ from the equilibrium position, i.e.,

$$\sigma(z,t)|_{z=\pm R}=P_{\pm}(t). \tag{30}$$

The restoring force of the surface is linked to both the surface tension and the variation of the surface area [3]. In the case of the slab there are no restoring forces on the surface and the pressure

$$P_{\pm}=0, \tag{31}$$

because the surface area does not change with surface shifts $\delta_{\pm}$. Note that boundary conditions (29)–(31) are the same as used in Secs. 6A-3a and 6A-3b in [3].

Let us substitute solutions (11) and (12) in the boundary conditions (29) and (30) and obtain the equation for the wave vector k:

$$\sigma(z,t)=\rho_\infty\frac{\delta\mathcal{E}(\rho)}{\delta\rho}=m\rho_\infty\left(a\xi(z,t)-d\frac{\partial^2\xi(z,t)}{\partial z^2}\right)$$
$$=\alpha\rho_\infty m(a+dk^2)\sin(\omega_0 t)\sin(kz+\varphi)|_{z=\pm R}=0. \tag{32}$$

Nontrivial solutions of this equation are

$$kR=\pi(n+1)\quad\text{for}\quad\varphi=0, \tag{33}$$

$$kR=\pi(n+1/2)\quad\text{for}\quad\varphi=\pi/2, \tag{34}$$

where $n=0,1,2,3,\ldots$. The value of the phase $\varphi=0$ should be omitted for the isoscalar oscillations of density in the slab, because the center of mass oscillates along the z axis at this phase value.

Now we determine the density vibrations amplitude by using Eqs. (14), (15), and relation $\omega=(\mathcal{C}/\mathcal{B})^{1/2}$ between the frequency ω, the mass $\mathcal{B}$, and the stiffness $\mathcal{C}$ parameters of the harmonic oscillator. After simple calculations of integrals in Eq. (15) we obtain

$$\alpha=\frac{\hbar}{(\mathcal{BC})^{1/2}}=\left(\frac{\hbar k}{m\rho_\infty RS(a+dk^2)^{1/2}}\right)^{1/2}, \tag{35}$$

where S is the unit square of the slab surface. Since we want our estimates to be meaningful for atomic nuclei, we define the value of S from the condition that the volume of vibrations in the slab is the same as the volume of nucleus with the mass number A_N.

For symmetric nuclear matter and the realistic Skyrme energy density functional, constants a_0, b_0, c_0, and d_0 are obtained as

$$a_0=2\rho_\infty\frac{\partial^2}{\partial\rho^2}\mathcal{E}_{Sk}|_{\nabla\rho^{p(n)}=0}$$
$$=\frac{(18\pi^4)^{1/3}\hbar^2}{3m}\rho_\infty^{2/3}+\frac{3t_0}{2}\rho_\infty+\frac{t_3}{8}(\alpha_0+2)(\alpha_0+1)\rho_\infty^{\alpha_0+1}$$
$$+\frac{(18\pi^4)^{1/3}}{6}[3t_1+t_2(5+4x_2)]\rho_\infty^{5/3}, \tag{36}$$

$$b_0=6\rho_\infty^2\frac{\partial^3}{\partial\rho^3}\mathcal{E}_{Sk}|_{\nabla\rho^{p(n)}=0}$$
$$=-\frac{(18\pi^4)^{1/3}\hbar^2}{3m}\rho_\infty^{2/3}+\frac{3t_3}{8}(\alpha_0+2)(\alpha_0+1)\alpha_0\rho_\infty^{\alpha_0+1}$$
$$+\frac{(18\pi^4)^{1/3}}{3}[3t_1+t_2(5+4x_2)]\rho_\infty^{5/3}, \tag{37}$$

$$c_0=12\rho_\infty^3\frac{\partial^4}{\partial\rho^4}\mathcal{E}_{Sk}|_{\nabla\rho^{p(n)}=0}$$
$$=\frac{8(18\pi^4)^{1/3}\hbar^2}{9m}\rho_\infty^{2/3}$$
$$+\frac{3t_3}{4}(\alpha_0+2)(\alpha_0+1)\alpha_0(\alpha_0-1)\rho_\infty^{\alpha_0+1}$$
$$-\frac{2(18\pi^4)^{1/3}}{9}[3t_1+t_2(5+4x_2)]\rho_\infty^{5/3}, \tag{38}$$

$$d_0=\frac{1}{32}[9t_1-t_2(5+4x_2)]\rho_\infty. \tag{39}$$

Here we have taken into account that the proton ρ^p and neutron ρ^n densities are connected to total density by expression $\rho^p(z,t)=\rho^n(z,t)=\frac{1}{2}\rho_\infty[1+\xi(z,t)]$ and the realistic Skyrme energy density functional in the Thomas-Fermi approach is defined as [18]

$$\mathcal{E}_{Sk}=\frac{3(9\pi^4)^{1/3}\hbar^2}{10m}[(\rho^p)^{5/3}+(\rho^n)^{5/3}]+\frac{1}{2}t_0\left[\left(1+\frac{1}{2}x_0\right)\rho^2 -\left(x_0+\frac{1}{2}\right)[(\rho^p)^2+(\rho^n)^2]\right]+\frac{1}{12}t_3\rho^{\alpha_0}\left[\left(1+\frac{1}{2}x_3\right)\rho^2 -\left(x_3+\frac{1}{2}\right)[(\rho^p)^2+(\rho^n)^2]\right]+\frac{3(9\pi^4)^{1/3}}{20}\left[t_1\left(1+\frac{1}{2}x_1\right) +t_2\left(1+\frac{1}{2}x_2\right)\right][(\rho^p)^{5/3}+(\rho^n)^{5/3}]\rho+\frac{3(9\pi^4)^{2/3}}{20}\left[t_2\left(x_2 +\frac{1}{2}\right)-t_1\left(x_1+\frac{1}{2}\right)\right][(\rho^p)^{8/3}+(\rho^n)^{8/3}]+\frac{1}{16}\left[3t_1\left(1 +\frac{1}{2}x_1\right)-t_2\left(1+\frac{1}{2}x_2\right)\right](\nabla\rho)^2-\frac{1}{16}\left[3t_1\left(x_1+\frac{1}{2}\right) +t_2\left(x_2+\frac{1}{2}\right)\right][(\nabla\rho^p)^2+(\nabla\rho^n)^2], \quad (40)$$

where $\rho=\rho^p+\rho^n$ and t_0, t_1, t_2, t_3, x_0, x_1, x_2, x_3, and α_0 are the Skyrme force parameters [17,18].

The values of constants a_0, b_0, c_0, d_0, and the parameters of most successful sets of Skyrme nucleon-nucleon interactions [19–22], the excitation energies of isoscalar density vibrations in the slab in the harmonic approximation $E=\hbar\omega_0$, the vibrations amplitudes α, and the ratios V_1 and W_{21} are shown in Table I. The energies, amplitudes, and ratios shown in Table I are calculated for two different values of slab thickness, which coincide with the diameters of nuclei with $A_N=40$ and $A_N=208$, respectively.

The values of constants a_0, b_0, c_0, and d_0 evaluated for different sets of Skyrme force are spread over wide intervals (see Table I). We can shorten these intervals if we know the experimental values of the ratio W_{21}. Unfortunately we do not have these data for the isoscalar resonances.

The anharmonicity of the one-phonon isoscalar monopole giant resonance obtained in [9] is consistent with the values summarized in Table I. The values of excitation energies calculated in the slab whose thickness is the same as the diameter of ^{208}Pb for different sets of Skyrme force agree with the experimental value of the isoscalar monopole resonance energy in ^{208}Pb $E\approx 13.2-13.9$ MeV [11].

The correctness of the definition of the unit square of surface S in Eq. (35) is supported by the proximity of the amplitude values presented in Table I and the amplitudes of vibrations evaluated for different microscopic and macroscopic models [6].

The anharmonicity is stronger in light nuclei than in the heavy ones because the vibration amplitudes in light nuclei are much larger than in the heavy ones, as we can see in Table I. Due to anharmonicity the excitation energies of the isoscalar one-phonon resonance $E_{1\hbar\omega}=\hbar\omega_0(1+V_1)$ are reduced by 5–10 % for heavy and by 12–30 % for light nuclei compared to the harmonic approach. Different sets of Skyrme interaction give various values of the ratios V_1 and W_{21}. The effect of the density vibrations anharmonicity for the Sk3 set of parameters of Skyrme force is lager than that obtained with other sets.

The dependence of the ratios V_1 and W_{21} on the values of constants a_0, b_0, c_0, and d_0 is shown in Figs. 1–4. The curves in this figures are calculated for the slab thickness which corresponds to the diameter of ^{208}Pb. We changed only one parameter and fixed others in each figure. We assume that the equilibrium density ρ_∞ does not change with the variations in parameters in Figs. 1–4. We choose the SkM* set of parameters of Skyrme force for fixed constants in Figs. 1–4.

The ratios V_1 and W_{21} are a linear function of the parameter c_0, and a quadratic function of b_0 [see Figs. 2, 3, and Eq. (22)]. The ratios V_1 and W_{21} are changed for large values of the constants a_0 and d_0 as $V_1\propto W_{21}\propto a_0^{1/2}$ and $V_1\propto W_{21}\propto d_0^{1/2}$. The dependence of the ratios V_1 on parameters b_0 and c_0 agrees with obtained in [23].

IV. ISOVECTOR EXCITATION

The isovector density vibrations in the slab are considered in similar way as the isoscalar oscillations in the previous section. Therefore we focus only on new features in this section.

Proton and neutron densities vibrate in the counter-phase in the case of the isovector excitations of density. The kinematic boundary conditions are defined separately for proton and neutron velocities in this case [8], i.e.,

$$v^p(z,t)|_{z=\pm R}=v^p_{S\pm}(t), \quad v^n(z,t)|_{z=\pm R}=v^n_{S\pm}(t). \quad (41)$$

The dynamic boundary condition requires that the normal to the surface pressure connected with deformation of isovector density in the slab volume be equal to the pressure of nuclear surfaces caused by restoring surface force,

$$\sigma(z,t)|_{z=\pm R}=P_\pm(t). \quad (42)$$

We assume that there is no isovector restoring force of surface in the approximation of the passive surface, i.e.,

$$P_\pm(t)=0. \quad (43)$$

The boundary conditions (41)–(43) are very similar to the boundary conditions for isoscalar density oscillations (29)–(31).

The eigenvalues of wave vector are determined by the equation

$$\sin(kz+\varphi)|_{z=\pm R}=0, \quad (44)$$

which is the same as Eq. (32). Equation (44) is solved in Eqs. (33),(34). The amplitude of isovector vibrations is also described by expression (35). In contrast to the isoscalar case for the isovector density vibrations we may choose two different phase values φ in Eq. (44): $\varphi=0$ and $\varphi=\pi/2$.

It would be useful to present proton and neutron densities in the symmetric nuclear matter for the isovector density oscillations as $\rho^p(z,t)=\frac{1}{2}\rho_\infty[1+\xi(z,t)]$, $\rho^n(z,t)=\frac{1}{2}\rho_\infty[1-\xi(z,t)]$. We substitute these expressions in Eq. (40) and

TABLE I. The parameters of Skyrme interaction, the constants of the energy density functional (3), the giant resonances energies in the slab evaluated in linear approach $E=\hbar\omega_0$, the density oscillations amplitudes α, and the ratios V_1 and W_{21} for different sets of Skyrme force. The energies values, amplitudes, and ratios V_1 and W_{21} are given for the two values of the slab thickness, which coincide with diameters of nuclei with $A_N=40$ and $A_N=208$. In the case of isovector excitations some quantities are presented for the two values of phases $\varphi=\pi/2$ and $\varphi=0$ (in parentheses).

	Sk3 [19]	Ska [20]	SkM* [21]	RATP [22]
t_0(MeV fm^3)	−1128.75	1602.78	−2645.00	−2160
t_1(MeV fm^5)	395.00	570.00	410.00	513.00
t_2(MeV fm^5)	−95.00	−67.00	135.00	121.00
t_3(MeV fm$^{3+3\alpha_0}$)	14000.00	8000.00	15595.00	11600.00
x_0	0.45	−0.02	0.09	0.418
x_1	0.00	0.00	0.00	−0.36
x_2	0.00	0.00	0.00	−2.29
x_3	1.00	−0.286	0.00	0.586
α_0	1.00	1/3	1/6	1/5
$\rho_\infty=3/(4\pi r_0^3)$(fm^{-3})	0.1453	0.1554	0.1603	0.1599
Isoscalar case				
a_0 (MeV)	79.06	58.58	48.17	53.33
b_0 (MeV)	733.5	459.8	347.4	401.5
c_0 (MeV)	46.53	−383.4	−424.2	−406.9
d_0 (MeV fm^2)	18.30	26.59	21.87	25.59
$R=r_0 208^{1/3}$				
$E=\hbar\omega_0$ (MeV)	12.9	11.5	10.5	11.1
α	0.039	0.042	0.045	0.044
V_1	−0.107	−0.050	−0.049	−0.047
W_{21}	0.952	0.977	0.977	0.978
$R=r_0 40^{1/3}$				
$E=\hbar\omega_0$ (MeV)	22.7	20.3	18.6	19.6
α	0.117	0.127	0.134	0.131
V_1	−0.330	−0.161	−0.160	−0.151
W_{21}	0.743	0.872	0.871	0.878
Isovector case				
a_0' (MeV)	112.6	131.7	120.2	117.1
b_0' (MeV)	0	0	0	0
c_0' (MeV)	240.2	326.6	270.05	305.6
d_0' (MeV fm^2)	4.949	7.988	5.485	−0.01129
$R=r_0 208^{1/3}$				
$E=\hbar\omega_0$ (MeV)	15.4 (30.9)	17.0 (34.2)	16.4 (32.9)	16.2 (32.3)
α	0.036 (0.051)	0.035 (0.050)	0.036 (0.051)	0.036 (0.051)
V_1	−0.028 (−0.014)	−0.018 (−0.009)	−0.025 (−0.012)	11.991 (5.99)
W_{21}	0.988 (0.988)	0.992 (0.992)	0.988 (0.989)	6.562 (6.563)
$R=r_0 40^{1/3}$				
$E=\hbar\omega_0$ (MeV)	26.7 (53.9)	29.6 (60.0)	28.5 (57.6)	28.0 (56.0)
α	0.108 (0.153)	0.105 (0.148)	0.109 (0.153)	0.109 (0.154)
V_1	−0.082 (−0.039)	−0.053 (−0.025)	−0.074 (−0.035)	36.0 (18.0)
W_{21}	0.936 (0.938)	0.958 (0.960)	0.941 (0.943)	29.9 (29.9)

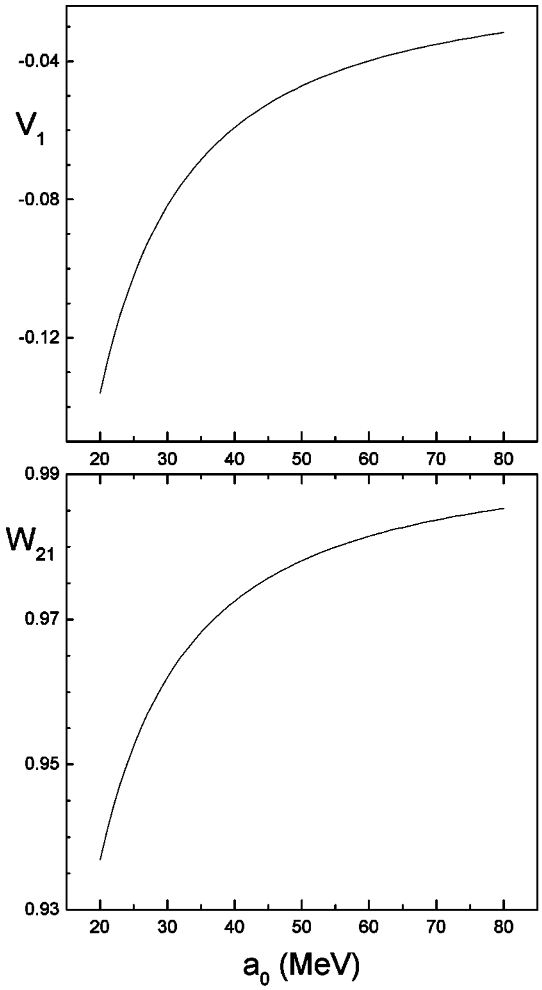

FIG. 1. Dependence of the ratios V_1 (top) and W_{21} (bottom) on a_0.

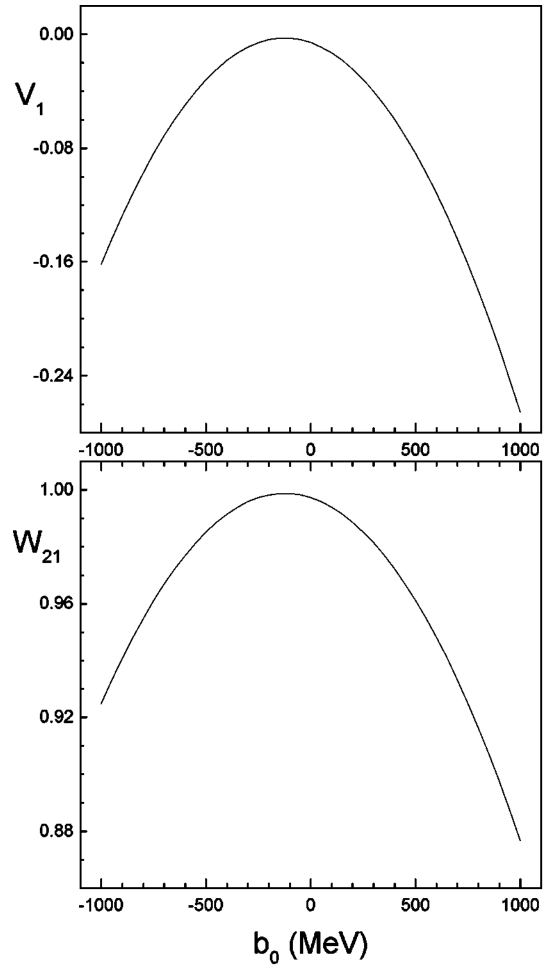

FIG. 2. Dependence of the ratios V_1 (top) and W_{21} (bottom) on b_0.

find the relationship between the constants a_0', b_0', c_0', and d_0' and parameters of Skyrme force

$$a_0'=\frac{(18\pi^2)^{1/3}\hbar^2}{3m}\rho_\infty^{2/3}+\frac{(18\pi^2)^{1/3}}{12}(t_2(4+5x_2)-3t_1x_1)\rho_\infty^{5/3} -t_0\rho_\infty\left(\frac{1}{2}+x_0\right)-\frac{1}{12}t_3(1+2x_3)\rho_\infty^{\alpha_0+1}, \tag{45}$$

$$b_0'=0, \tag{46}$$

$$c_0'=\frac{2(18\pi^2)^{2/3}}{9}\left(\frac{4\hbar^2}{m}\rho_\infty^{2/3}+(3t_1(1+x_1)+t_2(1-x_2))\rho_\infty^{5/3}\right), \tag{47}$$

$$d_0'=\frac{1}{16}\left[3t_1\left(x_1+\frac{1}{2}\right)+t_2\left(x_2+\frac{1}{2}\right)\right]\rho_\infty. \tag{48}$$

The constants a_0', b_0', c_0', and d_0' have the same meaning as in Eq. (3), but we denote them with a prime to distinguish the isoscalar and isovector constants.

The results of the calculation of the excitation energy, the amplitudes of the vibrations, and the ratios V_1 and W_{21} are presented in Table I for the same cases as for the isoscalar oscillations. We also calculated these quantities for the phase $\varphi=0$, which was not allowed for the isoscalar density oscillations.

The general tendencies of the anharmonic behavior of the isovector density vibrations are the same as for the isoscalar case. The new features are as follows.

(1) The RATP set of parameters of Skyrme force [22] shows an unrealistically strong anharmonicity of the isovector resonances. Our perturbative treatment of the nonlinear vibrations in Sec. II is not valid in this case. The values of ratios V_1 and W_{21} presented in Table I for the isovector oscillations for the RATP set can be interpreted qualitatively. We may conclude only that anharmonicity is very strong in this case. Such anharmonicity is not consistent with the experimental value $W_{21}=0.91\pm0.02$ [12] observed for electric giant dipole resonance, therefore it does not make much sense to use this set of Skyrme force parameters.

(2) The results for the ratio W_{21} are not very sensitive to the choice of phase $\varphi=0$ or $\varphi=\pi/2$, as we can see in Table I. In contrast to this the values of the ratio V_1 change approximately two times for different values of phase φ.

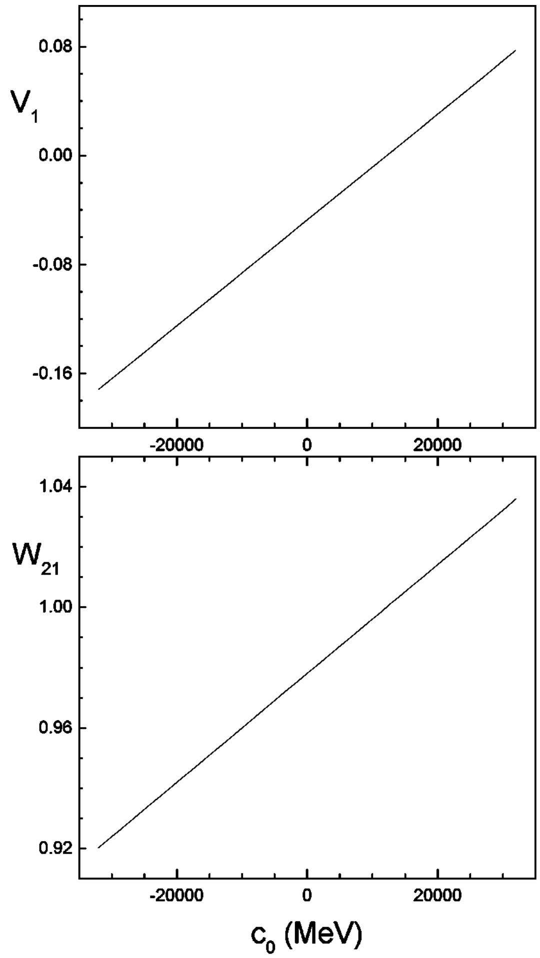

FIG. 3. Dependence of the ratios V_1 (top) and W_{21} (bottom) on c_0.

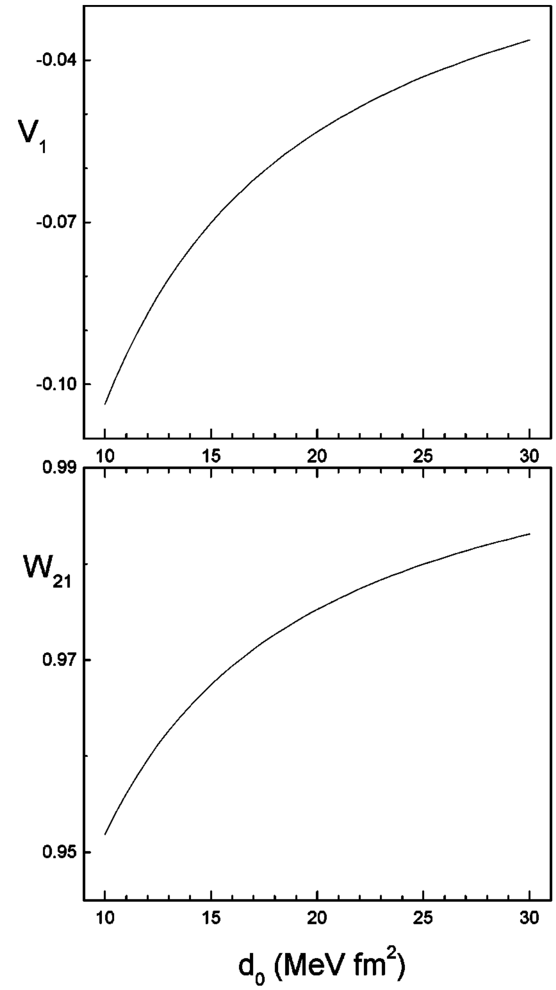

FIG. 4. Dependence of the ratios V_1 (top) and W_{21} (bottom) on d_0.

(3) We can conclude that the nonlinear effects for isovector oscillations are weaker than for isoscalar density vibrations in case of the sets Sk3, Ska, and SkM* of Skyrme interaction.

(4) The values of W_{21} calculated for the sets Sk3 and SkM* of Skyrme force agree well with the experimental value of $W_{21}=0.91\pm0.02$ [12] observed for the isovector giant dipole resonances. The anharmonicity of isovector giant resonances evaluated with the Ska set of Skyrme interaction is smaller than the experimental values. The anharmonicity obtained in Ref. [10] also agrees with values presented in Table I. Unfortunately it is difficult to make definite conclusion about the A_N dependence by using existing experimental data. Nevertheless the tendency of ratio W_{21} to increase with A_N is confirmed by experiment, see figures in [12,14].

V. CONCLUSION

The anharmonic terms of the energy density functional lower considerably the energy of the N-phonon excitation. Therefore the giant resonances should be studied in the framework of nonlinear models especially in light nuclei.

The experimental study of the N-phonon isoscalar and isovector giant resonances of different multipolarities gives us information about both the values and A_N dependence of the ratio W_{NM}. The additional experimental information may help to select sets of Skyrme force and reduce the variations of constants a_0, b_0, c_0, d_0, a_0', b_0', c_0', and d_0'. Note that only limited experimental information for one-phonon and two-phonon giant resonances is available for analysis [12,14]. Nevertheless we may conclude that the Sk3 and SkM* sets of Skyrme force lead to results which agree with experimental data of W_{21} for isovector giant resonances.

Unfortunately we do not have any data about the three-phonon giant resonances. Experimental data on the one-phonon, two-phonon, and three-phonon resonances may help greatly in determining the constants c_0 and c_0', because the role of these constants increase with the number of phonons N due to Eq. (26). The more precise definition of constants a_0, b_0, c_0, d_0, a_0', b_0', c_0', and d_0' should improve our knowledge about the equation of state and more accurate description of nuclear matter.

The study of the N-phonon giant resonances in hot nucleus provide information about the temperature dependence of the constants a_0, b_0, c_0, d_0, a_0', b_0', c_0', and d_0'.

[1] A. B. Migdal, Zh. Eksp. Teor. Fiz. **15**, 81 (1945).
[2] G. C. Baldwin and G. S. Klaiber, Phys. Rev. **71**, 3 (1947); **73**, 1156 (1948).
[3] A. Bohr and B. Mottelson, *Nuclear Structure* (Benjamin, New York, 1975), Vol. 2.
[4] J. P. Blazot, Phys. Rep. **64**, 171 (1980).
[5] F. E. Bertrand, Nucl. Phys. **A354**, 129 (1981).
[6] J. Speth and A. Van Der Woude, Rep. Prog. Phys. **44**, 720 (1981).
[7] V. M. Strutinsky, A. G. Magner, and V. Yu. Denisov, Sov. J. Nucl. Phys. **39**, 873 (1984); **42**, 690 (1984).
[8] V. Yu. Denisov, Sov. J. Nucl. Phys. **43**, 28 (1986); **44**, 20 (1986); **47**, 32 (1988); **49**, 38 (1989); **51**, 803 (1990).
[9] H. F. Boersma, R. Malfliet, and O. Scholten, Phys. Lett. B **269**, 1 (1991).
[10] D. Beaumel and Ph. Chomaz, Ann. Phys. (N.Y.) **213**, 405 (1992).
[11] S. Shlomo and D. H. Youngblood, Phys. Rev. C **47**, 529 (1993).
[12] H. Emling, Prog. Part. Nucl. Phys. **33**, 729 (1994).
[13] V. Yu. Ponomarev *et al.*, Nucl. Phys. **A569**, 333c (1994).
[14] E. Wajda *et al.*, Nucl. Phys. **A569**, 141c (1994).
[15] N. Frascaria, Nucl. Phys. **A569**, 111c (1994); **A583**, 63 (1995).
[16] L. D. Landau and E. M. Lifshits, *Hydrodynamics* (Nauka, Moscow, 1986).
[17] T. H. R. Skyrme, Nucl. Phys. **9**, 615 (1959).
[18] M. Brack, C. Guet, and H.-B. Hakansson, Phys. Rep. **123**, 275 (1985).
[19] M. Beiner, H. Flocard, N. V. Giai, and Ph. Quentin, Nucl. Phys. **A238**, 29 (1975).
[20] S. Kohler, Nucl. Phys. **A258**, 301 (1976).
[21] J. Bartel, Ph. Quentin, M. Brack, C. Guet, and H.-B. Hakansson, Nucl. Phys. **A386**, 79 (1982).
[22] M. Rayet, M. Arnould, F. Tondeur, and G. Paulus, Astron. Astrophys. **116**, 183 (1982).
[23] L. D. Landau and E. M. Lifshits, *Mechanics* (Nauka, Moscow, 1973).